Nipped-A regulates intestinal stem cell proliferation in *Drosophila*

Helen Marie Tauc[1],*, Alpaslan Tasdogan[2], Patrick Meyer[3] and Petra Pandur[1],*

ABSTRACT

Adult stem cells uphold a delicate balance between quiescent and active states, a deregulation of which can lead to age-associated diseases such as cancer. In *Drosophila*, intestinal stem cell (ISC) proliferation is tightly regulated and mis-regulation is detrimental to intestinal homeostasis. Various factors are known to govern ISC behavior; however, transcriptional changes in ISCs during aging are still unclear. RNA sequencing of young and old ISCs newly identified Nipped-A, a subunit of histone acetyltransferase complexes, as a regulator of ISC proliferation that is upregulated in old ISCs. We show that Nipped-A is required for maintaining the proliferative capacity of ISCs during aging and in response to tissue-damaging or tumorigenic stimuli. Interestingly, *Drosophila* Myc cannot compensate for the effect of the loss of Nipped-A on ISC proliferation. Nipped-A seems to be a superordinate regulator of ISC proliferation, possibly by coordinating different processes including modifying the chromatin landscape of ISCs and progenitors.

KEY WORDS: Aging, Intestine, Stem cell, Myc, Chromatin, TRRAP

INTRODUCTION

As a result of constant exposure to outside pathogens and harmful agents ingested with food, the gastrointestinal (GI) tract is inherently susceptible to a number of environmental insults throughout a lifetime. The functional and structural integrity of the intestinal epithelial lining is fundamental for normal GI function and is maintained and continually regenerated by adult stem cells. During aging, there is a progressive loss of intestinal homeostasis leading to impaired function and a higher probability of developing diseases such as cancer. One of the reasons for the loss of tissue homeostasis in mammals is speculated to be an altered stem cell behavior (Kirkwood, 2004; Saffrey, 2014); however, the exact effects of aging on the number and function of intestinal stem cells remains largely unclear. In recent years, *Drosophila* has become a prominent model organism to study mechanisms of regeneration and aging in the intestine (Jasper, 2015). Intestinal stem cells (ISCs) of the adult *Drosophila* midgut are vital for maintaining midgut homeostasis (Micchelli and Perrimon, 2006; Ohlstein and Spradling, 2006). A variety of mitogenic and stress signals induce a proliferative response in ISCs, which serves to replenish lost or damaged cells (Bonfini et al., 2016). During aging, *Drosophila* ISCs become hyperproliferative, resulting in tissue dysplasia (Biteau et al., 2008; Choi et al., 2008; Park et al., 2009). Studies have shown that chronic

inflammation within the midgut epithelium, promoted by a loss of symbiosis with commensal bacteria, results in elevated ISC proliferation, contributing to midgut dysplasia (Buchon et al., 2009; Guo et al., 2014). In contrast, limiting ISC proliferation during aging can significantly extend lifespan, signifying the importance of a balanced proliferative capacity of stem cells in maintaining intestinal homeostasis (Biteau et al., 2010; Guo et al., 2014; Rera et al., 2011; Wang et al., 2014).

In young, healthy flies, ISCs divide and generate a self-renewed ISC, which expresses the Notch (N) ligand Delta (Dl), and a post-mitotic progenitor cell called the enteroblast (EB). Upon division, Dl protein accumulates in the future ISC and is quickly downregulated in the EB, which in turn activates N signaling, initiating differentiation (Ohlstein and Spradling, 2007; Perdigoto et al., 2011). The EB differentiates into one of the two cell types of the gut, either into an enterocyte (EC) or an enteroendocrine (EE) cell. A substantial amount of work has shed light onto signaling pathways that regulate ISC proliferative activity in young flies including the EGFR, Insulin-like receptor (InR), p38 MAPK, Hippo, JAK/Stat and Jun-N-terminal kinase (JNK) signaling pathways (Biteau et al., 2011). In old flies, the molecules involved in perturbing the proliferative balance of ISCs remain to be fully elucidated. It is well accepted that, during aging, stem cells encounter both intrinsic and extrinsic changes. However, how stem cells adapt to cope with these changes, specifically in terms of altering epigenetic and transcriptional programs, remains an intriguing question. Endogenous transcriptional changes occurring in aged ISCs have not been studied in much detail in either the mammalian or *Drosophila* intestine. To address this question, we analyzed and compared the transcriptome of sorted cell populations enriched for ISCs from young and old *Drosophila* midguts. The data show an array of significant transcriptional changes in aged ISCs that provide first clues as to which genes hold important roles in the regulation of ISC behavior during aging.

Accumulating evidence suggests that changes in chromatin structure, including histone acetylation, are involved in the progression of aging (Feser and Tyler, 2011). However, to date, only few studies have investigated chromatin modifiers in the process of regulating ISC behavior in *Drosophila* (Amcheslavsky et al., 2014; Buszczak et al., 2009; Jin et al., 2013; Ma et al., 2013; Zeng et al., 2013). Nipped-A is the *Drosophila* homolog of mammalian transformation/transcription domain-associated protein (TRRAP) and yeast Tra1 and is an important subunit of histone acetyltransferase (HAT) complexes such as SAGA and Tip60 (Gause et al., 2006; Kusch et al., 2003; Murr et al., 2007). TRRAP/Tra1 is thought to function mainly as a scaffold for facilitating protein-protein interactions and recruiting various regulatory complexes to chromatin (Murr et al., 2007). Consistently, TRRAP has been shown to play a role in chromatin-based processes such as transcription, DNA repair and replication; however, its role in the context of aging remains to be investigated (Murr et al., 2007). The function and biological importance of *Drosophila* Nipped-A is largely uncharacterized on a tissue- and cell-specific level. So far it

[1]Institut für Biochemie und Molekulare Biologie, Universität Ulm, Albert-Einstein-Allee 11, Ulm 89081, Germany. [2]Institut für Immunologie, Universitätsklinikum Ulm, Albert-Einstein-Allee 11, Ulm 89081, Germany. [3]Institut für Dermatologie, Universität Ulm, Life Science Building N27, James Franck-Ring/Meyerhofstrasse 11c, Ulm 89081, Germany.

*Authors for correspondence (hmtauc@gmail.com; petra.pandur@uni-ulm.de)

P.P., 0000-0001-8973-5211

has only been shown that Nipped-A promotes N signaling activity in wing development (Gause et al., 2006).

Here, we identify Nipped-A as a newly discovered regulator of ISC proliferation during aging. Since Nipped-A transcripts were upregulated significantly in old ISCs, we knocked down *Nipped-A* in the ISCs and their progenitors to analyze the effects on midgut homeostasis. We show that reducing *Nipped-A* prevents the age-induced hyperproliferation of ISCs. Additionally, knocking down *Nipped-A* inhibits tumor growth induced by the small GTPase Ras as well as the proliferative response to tissue-damaging agents. Finally, we demonstrate that Nipped-A regulates global histone acetylation, thereby affecting chromatin-based processes that might also influence cell cycle regulation. Taken together, this work provides insight into transcriptional differences that potentially drive ISC aging and, with Nipped-A, uncovers a factor whose balanced expression is crucial for normal ISC proliferation.

RESULTS

Genetic changes in aging *Drosophila* ISCs

To identify genes that are important for regulating ISC aging, we examined endogenous changes in the transcriptome of young versus old ISCs. We isolated the ISCs by FACS according to our previously published protocol using the *esg*-GAL4, UAS-*GFP* fly line, in which GFP is expressed in both ISCs and EBs (Tauc et al., 2014; Yagi and Hayashi, 1997). In short, FACS analyses showed that the GFP$^+$ cells separate into two distinct populations based on GFP intensity and cell size. The cell population containing smaller, less granular cells with lower GFP intensity represents the population that is enriched for ISCs. Importantly, the distinct GFP expression profile of ISCs and EBs can be distinguished by FACS throughout aging (Tauc et al., 2014). For comparing the expression profile, we sorted cell populations enriched for ISCs from young (6-8 days old) and old (59-65 days old) midguts. Cells from three

different batches of young and old midguts were subjected to next-generation RNA sequencing (RNA-seq).

Results from the RNA-seq revealed that the expression of the majority of genes remained unchanged in old samples. Fig. 1A shows a Bland–Altman plot where genes whose expression changed at least twofold [false discovery rate (FDR) of <0.05] during aging are depicted in red. Out of the 8165 genes detected and sequenced, ~7% (580 genes) are significantly changed during aging (Fig. 1A). 73% of these genes are upregulated whereas 27% are downregulated (Fig. 1A). A gene ontology (GO) annotation analysis shows that the most overrepresented GO terms describe G-protein and neuropeptide signaling processes. The top ten of the enriched GO annotations are shown in Fig. 1B.

The genes that were identified by our RNA-seq analysis as being significantly differentially regulated during aging are attractive candidates to be studied further with respect to their function in aging. Of the top 40 most differentially expressed genes, we chose candidate genes that had a high counts per million (CPM) value, indicating a strong average expression. After an initial verification by qPCR and analyses of phenotypes after RNAi knockdown of different candidates, we chose to investigate Nipped-A because there is very little known about its function in *Drosophila*.

Nipped-A is required for the proliferative activity of ISCs and progenitor cells during aging

The RNA-seq results indicated an almost sixfold increase in *Nipped-A* mRNA transcripts in old ISCs compared with young ISCs. We confirmed a fourfold increase of *Nipped-A* mRNA transcripts by qPCR on FAC-sorted ISCs from young and old midguts (Fig. 1C). To examine the role of Nipped-A in ISCs and progenitor cells during aging, we used RNAi to knock down *Nipped-A* in *esg*-GFP$^+$ cells using the TARGET system (McGuire et al., 2003). We tested four *Nipped-A* RNAi fly lines and chose the

A

B

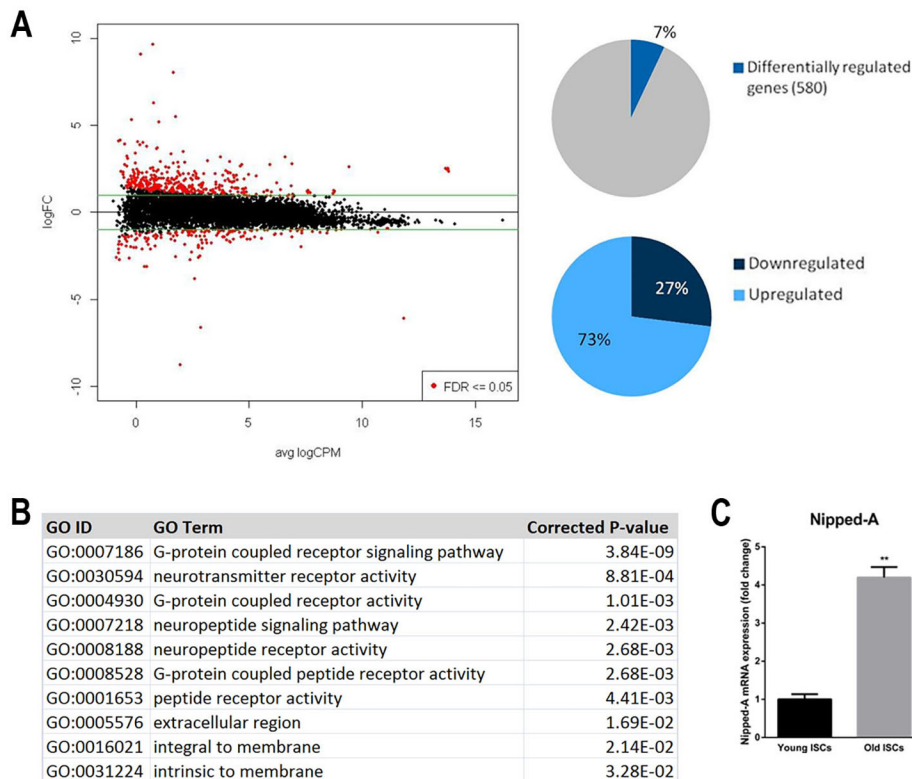| GO ID	GO Term	Corrected P-value
GO:0007186	G-protein coupled receptor signaling pathway	3.84E-09
GO:0030594	neurotransmitter receptor activity	8.81E-04
GO:0004930	G-protein coupled receptor activity	1.01E-03
GO:0007218	neuropeptide signaling pathway	2.42E-03
GO:0008188	neuropeptide receptor activity	2.68E-03
GO:0008528	G-protein coupled peptide receptor activity	2.68E-03
GO:0001653	peptide receptor activity	4.41E-03
GO:0005576	extracellular region	1.69E-02
GO:0016021	integral to membrane	2.14E-02
GO:0031224	intrinsic to membrane	3.28E-02

C

Fig. 1. Results from next-generation RNA sequencing. (A) A Bland–Altman plot representing the distribution of genes based on their fold-change (FC) and abundance, measured in counts per million (CPM) normalized counts. Genes exhibiting a significant change in expression, marked in red, were based on a false discovery rate (FDR) cutoff of 0.05. The horizontal lines demarcate a twofold difference in expression. The percentage of differentially expressed genes is depicted in the upper pie chart, and whether these were up- or downregulated is depicted in the lower pie chart. (B) Top ten GO terms that were enriched for in the RNA-seq. (C) Quantification of the increase in *Nipped-A* expression in ISCs during aging by real-time qPCR. RNA for qPCR was extracted from three biological replicates. The graph shows the mean±s.d. Statistical significance was calculated using the Student's *t*-test; **P=0.0045.

Nipped-A RNAi line TRiP #34849 to conduct all experiments in this study (Fig. S1). The expression of *Nipped-A* RNAi was induced in the *esg*-GFP^{+} cells in 6-8-day-old flies using *esg*-GAL4, UAS-CD8GFP, *tub*-GAL80[ts] (*esg[ts]*>*GFP*) by shifting the flies to 29°C. During aging, the percentage of *esg*-GFP^{+} cells in control midguts increased as expected. Knocking down *Nipped-A*, however, resulted in a progressive and significant loss of *esg*-GFP^{+} cells over time (Fig. 2A-E). Interestingly, in contrast to control flies, we observed a concomitant and significant decrease in the proportion of Dl^{+} cells within the *esg*-GFP[+] cell population after knocking down *Nipped-A* (Fig. 2F). Accordingly, we also observed a decrease in the proportion of cells with active N signaling over time as determined by using the *NRE*-mCherry N reporter fly line in combination with the *esg[ts]*>*GFP* fly line (Fig. 2G-L). After 4 days of *Nipped-A* RNAi expression, the percentage of cells active for N signaling was similar to the controls (Fig. 2G-H′,L). After 28 days we observed a significant increase in the proportion of N signaling-active cells in control midguts in addition to an overall increase in *esg*-GFP^{+} cells (Fig. 2I-L). This is consistent with a previous study showing an increase in N signaling in old midguts (Biteau et al., 2008). Knocking down *Nipped-A* for 28 days resulted in a significant reduction of cells that exhibited N signaling activity in

addition to the reduction of overall *esg*-GFP^{+} cells. Additionally, we performed this analysis using FACS as an unbiased method to measure the percentages of *esg*-GFP^{+} cells and *esg*-GFP[+]/*NRE*-mCherry^{+} cells from whole midguts after 4 and 28 days of *Nipped-A* RNAi expression. The results of the FACS analysis reflect the percentages of those counted manually in the posterior midgut (Fig. S2). Taken together, the results show that Nipped-A is required for maintaining ISCs and EBs during aging.

Nipped-A is required for ISC clone growth and differentiation
To further characterize the function of Nipped-A in ISCs, we used mosaic analysis with a repressible cell marker (MARCM) to analyze the nature of ISCs and their progeny after knocking down *Nipped-A*. Due to the close proximity of the *Nipped-A* gene to the centromere, we were unable to recombine genomic *Nipped-A* mutants into a corresponding FRT fly line and instead utilized the *Nipped-A* RNAi construct for reducing *Nipped-A* expression in MARCM clones. GFP-marked clones in the posterior half of the midguts were analyzed 3, 7, 14 and 28 days after clone induction (ACI). Three days ACI, the majority of both control and *Nipped-A* RNAi clones contained one or two cells. Over time, the size of control clones increased, resulting in a higher number of clones containing 3-5
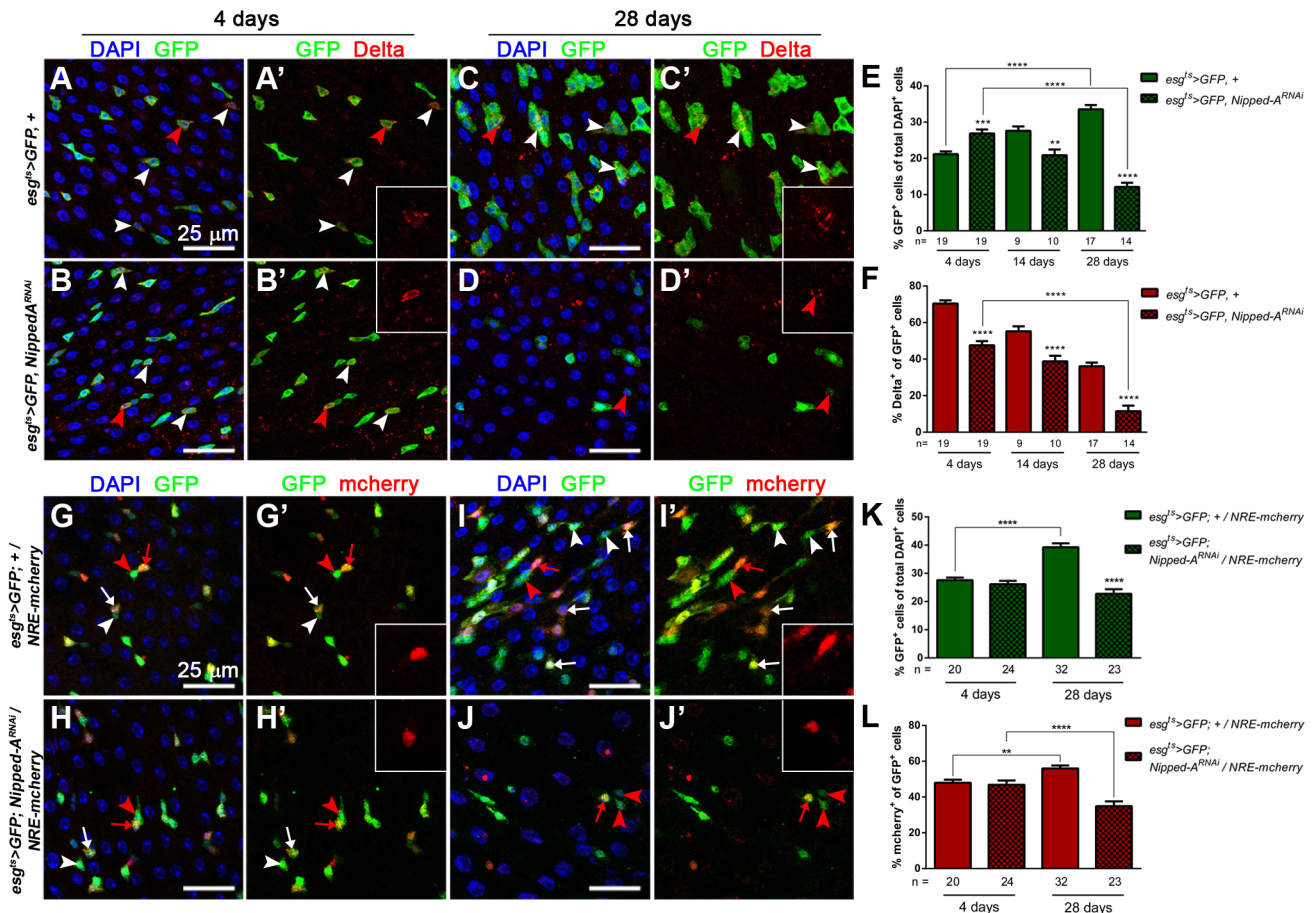

Fig. 2. Knocking down *Nipped-A* results in fewer *esg*-GFP^{+} cells and decreased Notch signaling during aging. (A-D) Immunostaining for GFP and Delta in the posterior midgut at 4 days (A-B′) and 28 days (C-D′) at 29°C. White arrowheads point to Delta^{+} cells. Red arrowheads point to the cell that is enlarged in the inset. (E,F) The percentage of *esg*-GFP^{+} cells of the total DAPI^{+} cells counted (E) and the proportion of Delta^{+} cells within the *esg*-GFP[+] cell population (F). (G-J′) Immunostaining for GFP and the Notch reporter *NRE*-mCherry at 4 days (G-H′) and 28 days (I-J′) at 29°C. All arrowheads point to *esg*-GFP[+]/mCherry^{−} cells and all arrows point to *esg*-GFP[+]/mCherry^{+} cells. Red arrowheads/arrows point to the cells that are enlarged in the inset. (K,L) The percentage of *esg*-GFP^{+} cells of the total DAPI^{+} cells counted (K) and the proportion of *esg*-GFP[+]/mCherry^{+} cells within the *esg*-GFP[+] cell population (L). The graphs show the mean±s.e.m. Statistical significance was calculated using the Student's *t*-test; **P<0.01, ***P<0.0005, ****P<0.0001. Asterisks directly above bars indicate a significant difference between this bar and the adjacent control bar to the left. See also Figs S1 and S2.

cells or ≥6 cells per clone. In contrast, the majority of *Nipped-A* RNAi clones remained single-cell clones at all time points (Fig. 3A-E). Starting at 7 days ACI, ~20% of the *Nipped-A* RNAi clones contained two cells and 10% of the clones contained 3-5 cells. Only a very low percentage of clones grew and contained six or more cells. This result suggests that *Nipped-A* RNAi ISC clones have a restricted capacity to divide and generate progeny. Notably, clones expressing *Nipped-A* RNAi were still present after 28 days ACI, implying that Nipped-A is not required for cell survival.

To determine how many cells within each clone were stem cells or stem cell-like, we analyzed Dl expression. An ISC can divide asymmetrically to produce a renewed Dl$^+$ stem cell and an EB (Dl$^-$), or symmetrically to produce either two Dl$^+$ stem cells or two EBs (de Navascues et al., 2012; O'Brien et al., 2011). We analyzed Dl expression in clones at 7 days ACI and found that for single-cell clones, the number of clones that were Dl$^+$ (~30%) did not differ between control and *Nipped-A* RNAi clones (Fig. S3). The majority of the control clones that contained 2-5 cells had one Dl$^+$ cell per clone, indicating that most ISC divisions occur asymmetrically (Fig. 3F,F′,J). In contrast, the proportion of clones that had either no Dl$^+$ or two Dl$^+$ cells increased when *Nipped-A* was knocked down (Fig. 3G,G′,J). The increase of clones containing no Dl$^+$ cell

demonstrates that *Nipped-A* is required for maintaining ISC identity. This finding also correlates with the loss of Dl$^+$ cells we observed upon knocking down *Nipped-A* in the *esg*-GFP$^+$ cells (see Fig. 2F). The increased proportion of clones containing either two Dl$^+$ cells or none after *Nipped-A* knockdown could be due to an altered binary fate decision, resulting in an increase in symmetrical divisions. However, most *Nipped-A* RNAi clones remained single cells, a significant portion of which expressed Dl. Therefore, we hypothesized that Nipped-A has a more important role in the ability of ISCs to proliferate than in its binary fate decision.

Since the majority of *Nipped-A* RNAi clones remained small single cells over time, 70% of which were Dl$^-$ at 7 days ACI, we addressed the possibility that they had directly differentiated into EE cells. Therefore, we analyzed the EE cell marker Prospero (Pros) and found that at 7 days ACI, there were significantly fewer *Nipped-A* RNAi clones that contained a Pros$^+$ cell (Fig. 3H-I′,K). From these results we conclude that *Nipped-A* RNAi clones do not differentiate into EE cells. We also analyzed whether *Nipped-A* RNAi clones can differentiate into ECs. For this analysis, we defined ECs as having a nuclear diameter of more than 7 μm (Bardin et al., 2010). The majority of single- and two-cell clones did not contain a large EC-like cell in both control and *Nipped-A* RNAi
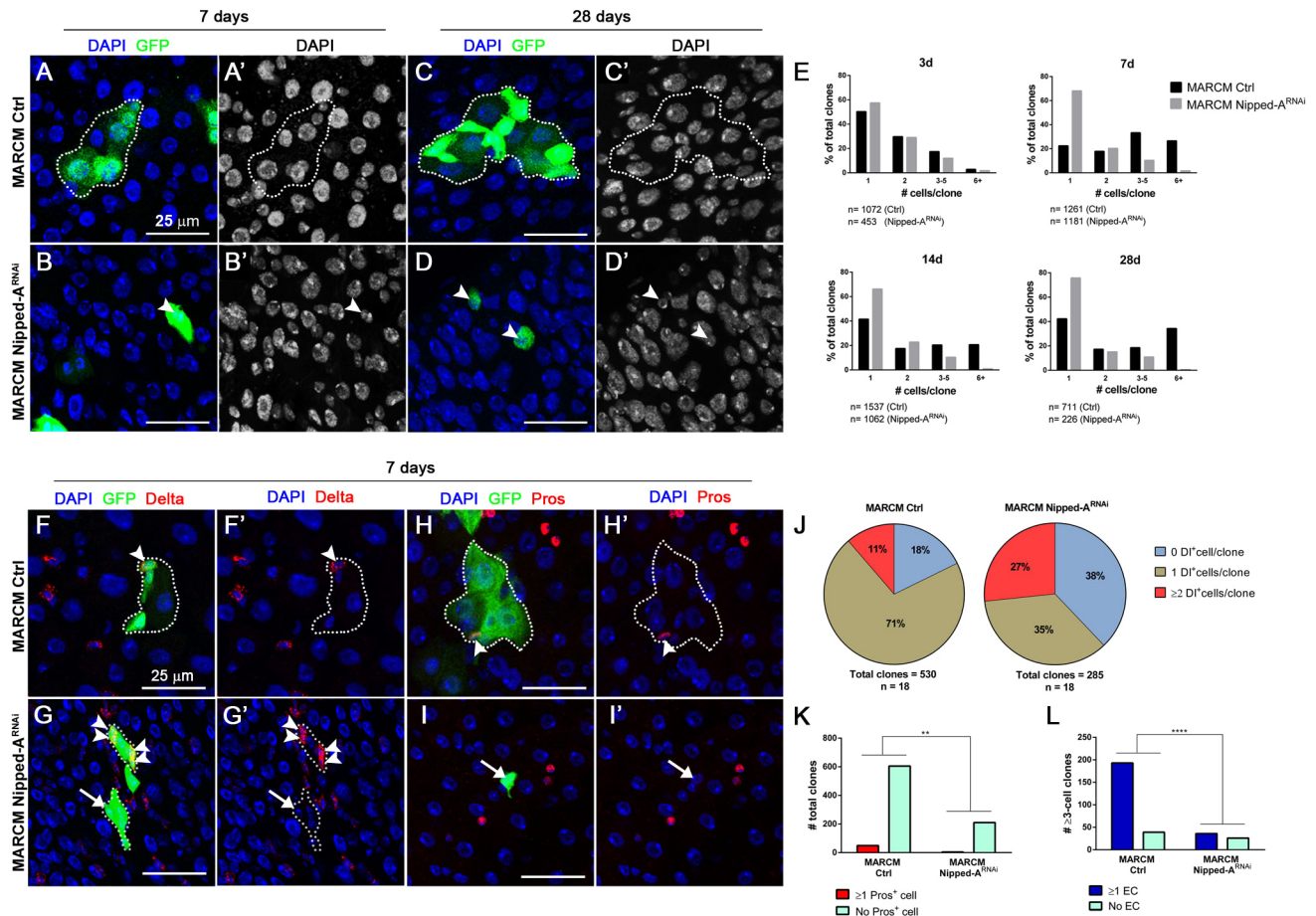

Fig. 3. Clonal analyses show a role for *Nipped-A* in proliferation and differentiation at 7 days ACI. (A-D′) A comparison of MARCM control clones with MARCM *Nipped-A* RNAi clones at 7 days (A-B′) and 28 days (C-D′) ACI. Arrowheads in B-D′ point to single cell clones, dotted outline depicts individual MARCM clones. (E) Quantification of clonal size based on the number of cells per clone at 3 days, 7 days, 14 days and 28 days ACI. (F-I′) Immunostaining for GFP and Delta (F-G′) or Pros (H-I′) in MARCM control versus MARCM *Nipped-A* RNAi clones at 7 days. Arrowheads in F-G′ point to Delta$^+$ cells and the arrow points to a clone that lacks Delta$^+$ cells. The arrowhead in H,H′ points to a Pros$^+$ cell. In I,I′ the arrow points to a Pros$^-$ cell clone. Dotted outline depicts individual MARCM clones. (J) Pie charts showing the proportion of clones (consisting of 2-5 cells) that contained one Dl$^+$ cell (beige), two or more Dl$^+$ cells (red) and no Dl$^+$ cell (blue). (K) Quantification of the number of clones in which at least one cell differentiated into a Pros$^+$ EE. (L) Quantification of the number of clones (containing three or more cells) that have at least one EC. Statistical significance was tested using the Chi square test in K,L; **P<0.005, ****P<0.0001. See also Fig. S3.

clones (Fig. S3). For clones that contained three or more cells, we observed that there were significantly fewer clones with an EC-like cell after knocking down *Nipped-A* (Fig. 3L).

In summary, our observations suggest that Nipped-A can regulate ISC identity and is required for progenitor differentiation. Importantly, the clonal analysis strongly suggests a cell-autonomous role for Nipped-A in regulating ISC proliferation.

Nipped-A is required for ISC proliferation

Knocking down *Nipped-A* in either the *esg*-GFP$^+$ progenitor cells in whole midguts or in clones resulted in a decrease of *esg*-GFP$^+$ cells and small clone size during aging. To determine whether Nipped-A is required for normal proliferation of the ISCs, we performed EdU incorporation assays after 4 and 28 days of *Nipped-A* RNAi expression using *esg^{ts}>GFP* and quantified the number of phosphorylated histone 3 (PH3)-positive cells per midgut. After 4 days of *Nipped-A* RNAi expression, the number of EdU$^+$ cells and

the number of PH3$^+$ cells per midgut was higher than in controls (Fig. 4A-B′,E). This observation suggests that Nipped-A might be required for maintaining ISC quiescence under homeostatic conditions in young flies. We tested three additional *Nipped-A* RNAi lines to verify the increase of EdU$^+$ cells at four days (Fig. S4). We found that only one RNAi line had this effect in this assay and interestingly, also revealed potential regional differences. Hence, this observation should be interpreted with caution. After 28 days of *Nipped-A* RNAi expression, the number of EdU$^+$ cells as well as the number of PH3$^+$ cells per midgut decreased significantly (Fig. 4C-E).

To exclude the possibility that the *esg*-GFP$^+$ cells undergo apoptosis after knocking down *Nipped-A*, we performed TUNEL assays and analyzed posterior midguts after 4 and 28 days of *Nipped-A* RNAi expression (Fig. 4F-I′). We did not observe a notable difference in the number of apoptotic *esg*-GFP$^+$ cells between the posterior midguts of control flies and after knocking down *Nipped-A*
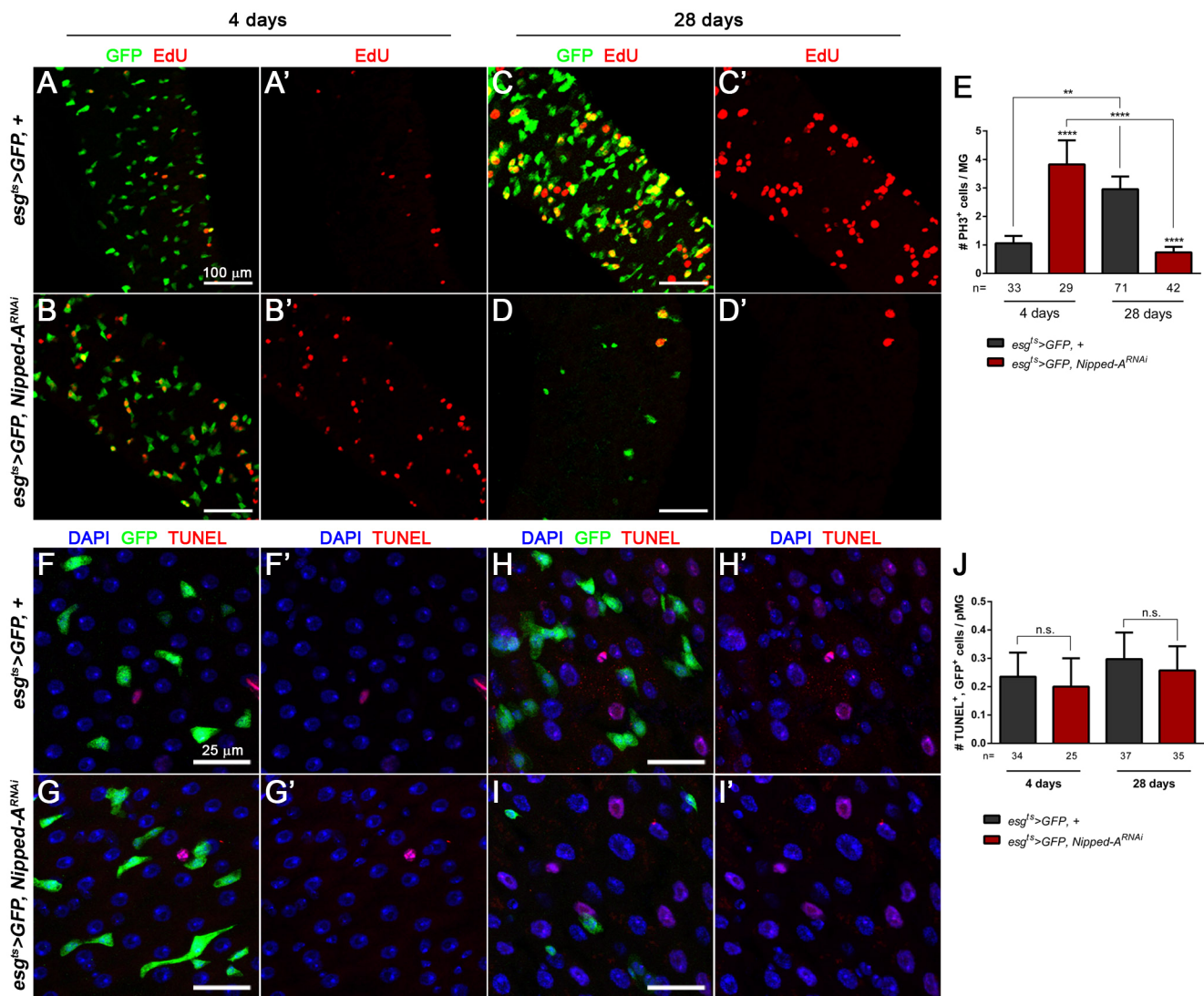

Fig. 4. Reducing *Nipped-A* leads to a loss of progenitor cells due to decreased proliferation but not an increase in apoptosis. (A-D′) EdU incorporation within the last 24 h before analysis at 4 days (A-B′) and 28 days (C-D′) at 29°C. (E) Quantification of the number of PH3$^+$ cells per midgut (MG) at 4 days and 28 days at 29°C. (F-I′) TUNEL assay performed at 4 days (F-G′) and 28 days (H-I′) at 29°C. (J) Quantification of the number of *esg*-GFP$^+$ cells that were also TUNEL$^+$ in the posterior midgut (pMG) at 4 days and 28 days at 29°C (n.s., not significant). The graphs show the mean±s.e.m. Statistical significance was calculated using the Student's *t*-test; **P<0.01, ****P<0.0001. Asterisks directly above bars indicate a significant difference between this bar and the adjacent control bar on the left. See also Figs S4 and S5.

(Fig. 4J). As a positive control we used midguts dissected from bleomycin-fed flies, which exhibited a prominent increase in apoptotic cells as compared with the sucrose-fed controls (Fig. S5). These results indicate that the observed loss of *esg*-GFP$^+$ cells after knocking down *Nipped-A* is not due to an increase in apoptosis. Taken together, the results demonstrate a requirement for Nipped-A in maintaining the proliferative activity of ISCs during aging.

Deregulated proliferation is one of the hallmarks of tumor formation. Tumor formation in the midgut can be induced genetically, for example by overactivating the mitogenic EGFR signaling pathway or inhibiting N signaling (Ohlstein and Spradling, 2007; Jiang et al., 2011; Biteau and Jasper, 2011). Thus, we asked whether manipulating these pathways in the ISCs and progenitor cells could overcome the loss of proliferation after *Nipped-A* knockdown. Knocking down *N* using *N* RNAi in *esg*-GFP$^+$ cells leads to tumors consisting of ISCs and EEs after 14 days. Knocking down both *Nipped-A* and *N* in the *esg*-GFP$^+$ cells notably decreased the formation of tumors after 14 days (Fig. S6). Hence,

Nipped-A is required for the proliferative response of the ISCs after blocking N signaling.

Next, we expressed a construct of the small GTPase Ras that is constitutively active, UAS-*Ras*^{ACT} (hereafter *Ras*^{ACT}), using *esg*^{ts}>*GFP* to activate EGFR signaling in the progenitor cells. After 4 days of expressing *Ras*^{ACT}, we observed robust ISC proliferation and *esg*-GFP$^+$ cell accumulation (Fig. 5A,A′,C). When *Nipped-A* RNAi was co-expressed with *Ras*^{ACT}, ISC proliferation was dramatically reduced after only 4 days of co-expression (Fig. 5B,C). After 14 days of co-expressing *Ras*^{ACT} and *Nipped-A* RNAi, there were only a few remaining *esg*-GFP$^+$ cells within the entire midgut (Fig. 5D-E″). Additionally, we noticed that many of the *esg*-GFP$^+$ cells were larger in size and had large nuclei (arrows in Fig. 5B,B′). This is an interesting observation because Ras is known to be involved in cell growth (Prober and Edgar, 2000). Thus, cell growth induced by Ras does not seem to be influenced by the loss of *Nipped-A*, suggesting a specific role for Nipped-A in cell division. Taken together, these observations led us
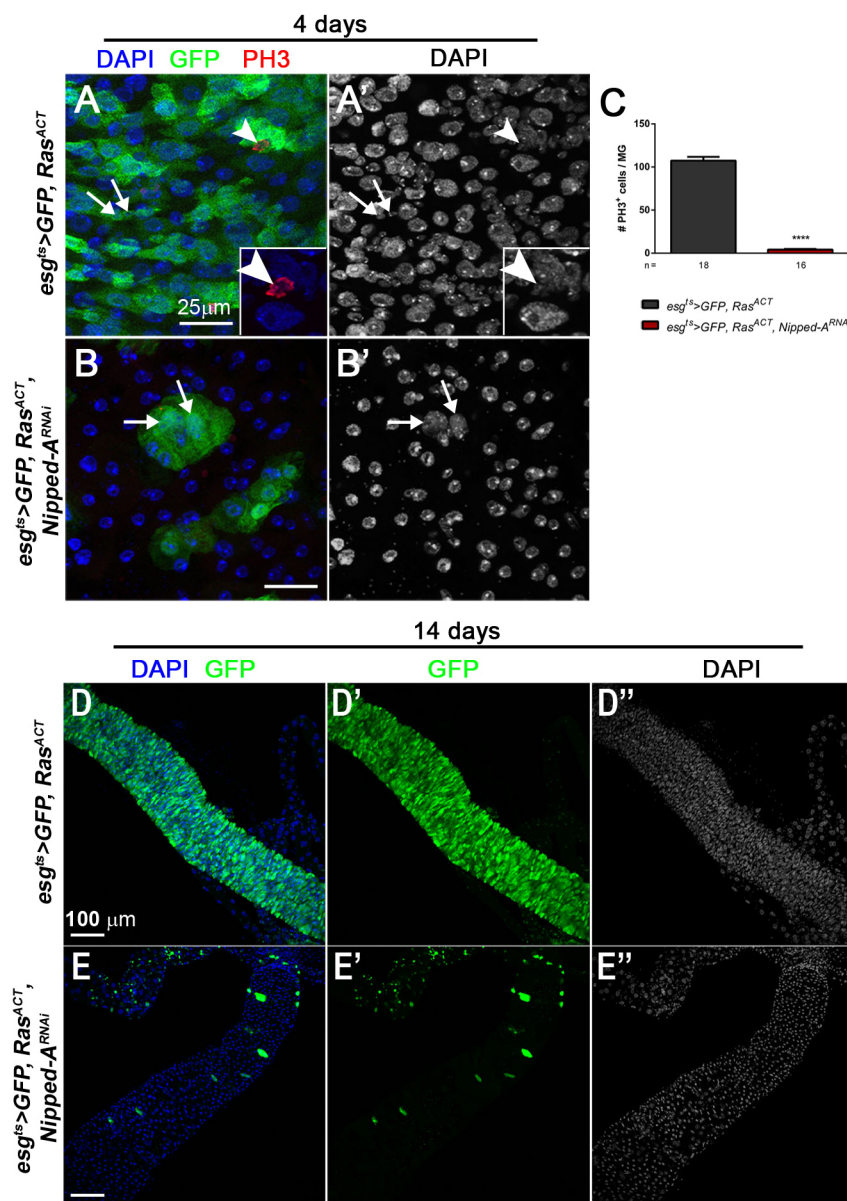

Fig. 5. Nipped-A is required in precursor cells for ISC proliferation upon Ras overactivation. (A-B′) Immunostaining for PH3 and GFP after 4 days of *Ras*^{ACT} overexpression (A,A′) or *Ras*^{ACT} overexpression and concomitant *Nipped-A* knockdown (B,B′). The arrows in A-B′ point to *esg*-GFP$^+$ cell nuclei; note the difference in nuclear size. Arrowheads in A,A′ point to a PH3$^+$ cell. (C) Quantification of PH3$^+$ cells per midgut (MG) after 4 days of transgene induction. The graph shows the mean±s.e.m. Statistical significance was calculated using the Student's *t*-test (****P<0.0001). Asterisks directly above bars indicate a significant difference between this bar and the adjacent control bar on the left. (D-E″) Immunostaining for GFP after 14 days of *Ras*^{ACT} overexpression alone (D-D″) or in combination with *Nipped-A RNAi* (E-E″). See also Fig. S6.

to conclude that Nipped-A is essential for ISC proliferation during aging and upon tumorigenic stimulation.

Myc cannot rescue the proliferation defect in the absence of Nipped-A

We next asked whether Nipped-A is also necessary for ISC proliferation during midgut regeneration. Dextran sulfate sodium (DSS) and bleomycin cause a strong proliferative response in ISCs upon ingestion. DSS was shown to affect ISCs through disrupting the basement membrane and acting through the Hippo pathway effector Yorkie in ISCs and EBs (Amcheslavsky et al., 2009; Ren et al., 2010). The DNA-damaging agent bleomycin has been shown to act primarily in the ECs, triggering ISC proliferation via JAK/STAT and EGFR signaling pathways (Amcheslavsky et al., 2009; Ren et al., 2010). The signaling pathways that are activated by DSS and bleomycin and mediate the response to both chemicals converge on and require *Drosophila* Myc in the progenitor cells (Cordero et al., 2012; Ren et al., 2013). To assess the capacity of ISCs to respond to these agents, flies at 4 days of *Nipped-A* RNAi expression were fed either a 5% sucrose solution or 5% sucrose solution containing 5% DSS or 25 µg/ml bleomycin for two days. As expected, quantification of the PH3$^+$ cells per midgut showed that the ISCs in control midguts mounted a strong proliferative response to both chemical agents (Fig. 6A, gray bars). Reducing *Nipped-A* expression in ISCs resulted in a strong decrease in proliferative cells compared with controls as early as 4 days (Fig. 6A, red bars). These results indicate an important role for Nipped-A in the *esg*-GFP$^+$ cells not only for maintaining ISCs over time, but also for the proliferative response induced by tissue-damaging agents in young flies.

As Myc has a pivotal role in the response to tissue damage as well as in normal ISC maintenance and proliferation, we asked whether overexpressing *Myc* could rescue the *Nipped-A* RNAi phenotype in tissue regeneration and during aging. Interestingly, this was not the case. Co-expression of *Myc* and *Nipped-A* RNAi did not rescue the ISC proliferation defect caused by knocking down *Nipped-A* in response to DSS or bleomycin (Fig. 6A, green bars). Of note, overexpression of *Myc* alone in the *esg*-GFP$^+$ cells did not further augment the proliferative response of ISCs upon DSS or bleomycin treatment as measured by the number of PH3$^+$ cells per midgut (Fig. 6A, blue bars). Consistently, overexpressing *Myc* alone for 30 days resulted in similar numbers of *esg*-GFP$^+$ cells as in the control midguts (Fig. 6B,B′,D,D′). Also in aged midguts, co-expressing *Myc* and *Nipped-A* RNAi did not rescue the loss of *esg*-GFP$^+$ cells caused by reduced *Nipped-A* (Fig. 6C,C′,E,E′). Since the mammalian homolog of Nipped-A, TRRAP, can bind MYC and was shown to facilitate MYC binding to chromatin and activating target genes, including cell cycle genes (Bouchard et al., 2001; Frank et al., 2001; Liu et al., 2003; McMahon et al., 1998; Park et al., 2001), we used qPCR to test whether knocking down *Nipped-A* affects the transcriptional function of Myc by analyzing the expression of several Myc targets in sorted *esg*-GFP$^+$ cells. Unexpectedly, not only was the expression of *Myc* itself significantly upregulated after knocking down *Nipped-A*, several of its target genes including *Cdk4*, *Rbf*, *Taf60-2* (also known as *mia*) and *HP1b* were also upregulated (Orian et al., 2003) (Fig. 6F). Other Myc target genes involved in the cell cycle included *Cyclin A* and *Cyclin B*, the expression of which remained unchanged. These results indicate that the transcriptional activity of Myc in regulating cell cycle gene expression seems to be unchanged or even upregulated. Additionally, we examined cell cycle regulators such as *Cyclin D*, *Cyclin E* and *mad2*, most of which were upregulated

upon *Nipped-A* knockdown (Fig. 6F). Taken together, the expression of most of the tested Myc targets, as well as other cell cycle genes, were significantly upregulated after knocking down *Nipped-A*. Thus, our findings indicate that the defect in cell division is independent of the transcriptional activity of these genes and is due to an effect of reduced *Nipped-A* downstream or parallel to Myc.

Nipped-A modulates global acetylation of H3 and H4

As Nipped-A was identified to be a component of HAT complexes such as the Tip60 and the SAGA complex in *Drosophila* (Kusch et al., 2003), we hypothesized that reducing *Nipped-A* affects histone acetylation in midgut progenitor cells. To test this, we investigated the global acetylation status of histone 3 (H3) and histone 4 (H4) (Fig. 7). Upon analyzing the staining intensity of H3Ac and H4Ac in *esg*-GFP$^+$ cells, we observed that at 14 and 28 days of *Nipped-A* knockdown, there is a reduction of H3Ac and H4Ac. The reduction of staining intensity for H3Ac was more pronounced (~50-60% lower than controls) compared with the reduction of staining intensity for H4Ac (~30% lower than controls) (Fig. 7E,J). In addition, we tested the acetylation status of H3K27 (Fig. S7), an active histone mark that has been associated with increased proliferation in colon cancer and deregulated Ras signaling (Karczmarski et al., 2014; Nabet et al., 2015). Strikingly, knocking down *Nipped-A* led to a dramatic decrease in H3K27Ac after 14 and 28 days (Fig. S7). These data support a role for Nipped-A in maintaining the global acetylation status of H3 and H4 in ISCs during aging, including acetylation marks that are potentially important for regulating the proliferative capacity of ISCs.

DISCUSSION

Loss of tissue integrity and function is a detrimental process affecting the health of individuals during aging. In *Drosophila*, the aging midgut epithelium is characterized by ISC hyperproliferation accompanied by EB mis-differentiation and tissue dysplasia (Biteau et al., 2008). Our RNA-seq analysis aimed to identify endogenous changes in the transcriptome profiles of young and old ISCs. The results uncovered 580 differentially regulated genes that are potentially important in maintaining ISC integrity and function throughout aging. Among the differentially expressed genes, *Nipped-A* transcripts were significantly upregulated in aged ISCs. The only previous study exploring the function of Nipped-A in *Drosophila* showed that it positively regulates N signaling in wing development (Gause et al., 2006). Interestingly, our findings do not support a role for *Nipped-A* in promoting N signaling in midgut ISCs as knocking down *Nipped-A* did not phenocopy the *N* loss-of-function phenotypes. This indicates that Nipped-A most likely functions differently on a molecular level depending on the cellular context. We did observe a gradual decrease in both Dl$^+$ cells and cells active for N signaling within the *esg*-GFP$^+$ cell population after knocking down *Nipped-A*. This effect can be attributed to a loss of ISC maintenance and/or identity over time as well as to the loss of proliferative capacity after *Nipped-A* reduction.

Since the RNAi knockdown of *Nipped-A* prevented the age-induced hyperproliferation of ISCs, our findings indicate that the endogenous upregulation of *Nipped-A* in old ISCs contributes to the hyperproliferation of ISCs in aged midguts. We further propose that Nipped-A is required for preserving ISC integrity under elevated stress conditions, which also occur during aging. This conclusion is supported by reduced EdU incorporation over time and reduced numbers of mitotic cells after challenging midguts with stress-inducing chemicals upon *Nipped-A* reduction. Furthermore, the
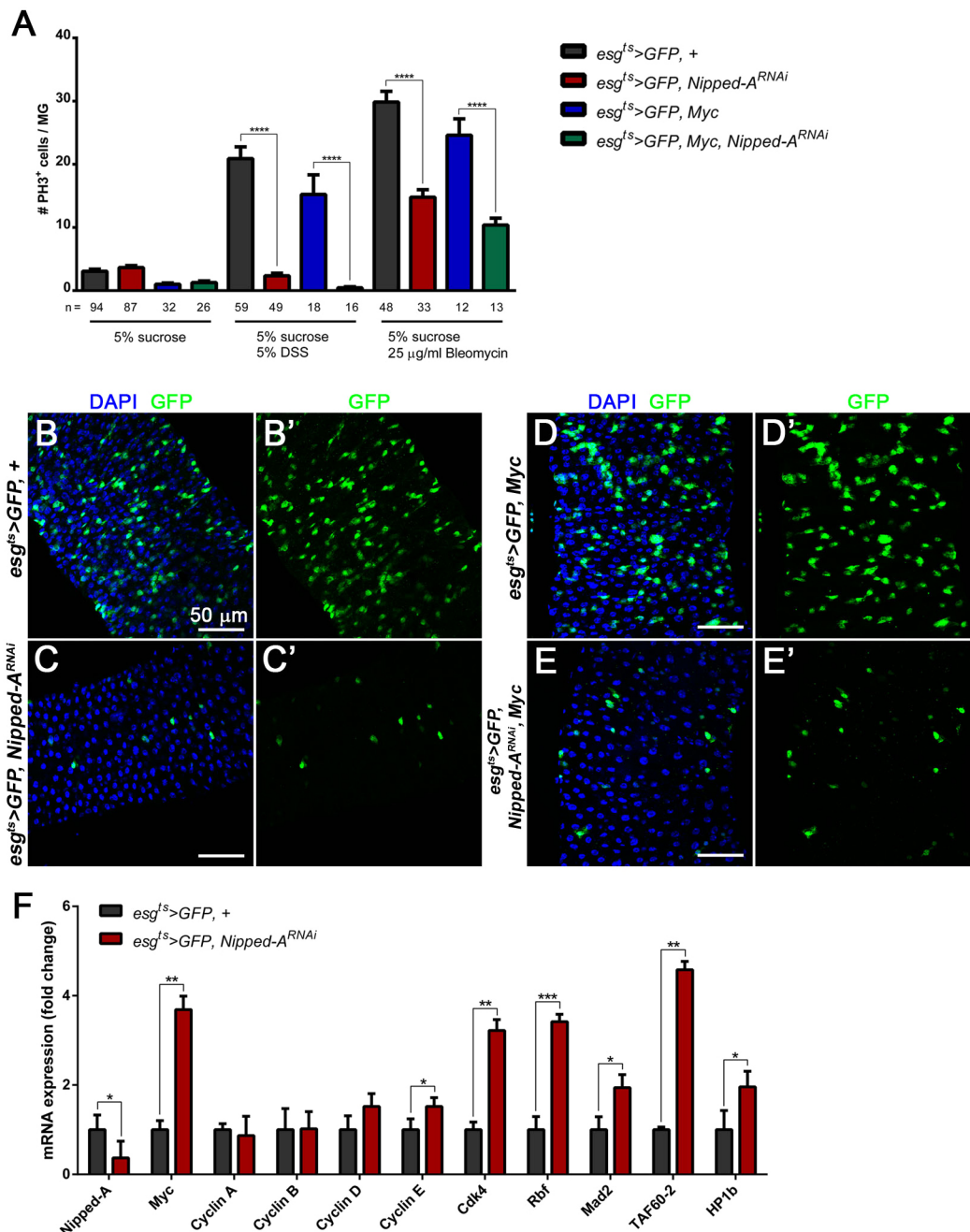
Fig. 6. *Myc* overexpression is insufficient to rescue the *Nipped-A* RNAi phenotype in response to tissue damage and during aging. (A) Quantification of PH3+ cells per midgut (MG) after 48 h of treatment with either DSS or bleomycin at 4 days of transgene induction. (B-E′) Immunostainings for GFP in controls (B,B′), after *Nipped-A* RNAi expression (C,C′), after *Myc* overexpression (D,D′) and after *Myc* and *Nipped-A* RNAi co-expression (E,E′) for 30 days. (F) Comparison of gene expression between sorted control and *Nipped-A RNAi*-expressing *esg*-GFP+ cells, 13-16 days after RNAi induction, *n*=3 independent batches of cells. The graphs show the mean±s.e.m. (A) or mean±s.d. (F). Statistical significance was calculated using the Student's *t*-test; *$P<0.05$, **$P<0.005$, ***$P<0.001$, ****$P<0.0001$.

dramatic hyperproliferation of ISCs induced by activating Ras signaling or by inhibiting N signaling was essentially abolished when *Nipped-A* was reduced. The effect of knocking down *Nipped-A* does not seem to be specific to a particular signaling pathway; therefore, Nipped-A regulates either a crucial factor or a global mechanism to allow proliferation.

Taking into account the versatility of Myc function, and particularly its importance in ISC cell division (Ren et al., 2013), we tested whether overexpressing *Myc* could rescue the *Nipped-A* RNAi phenotype. Overexpression of *Myc* failed to rescue the

proliferation defect caused by knocking down *Nipped-A*, suggesting that Nipped-A elicits its function downstream of or parallel to Myc. Interestingly, although Myc was shown to be essential for proliferation in ISCs, overexpression of *Myc* alone did not induce ISC overproliferation (Ren et al., 2013). This finding is consistent with our data showing that overexpression of *Myc* does not further enhance the proliferative response of the cells to tissue-damaging reagents.

Mammalian TRRAP is known to bind MYC (McMahon et al., 1998; Park et al., 2001) and the recruitment of HAT complexes by
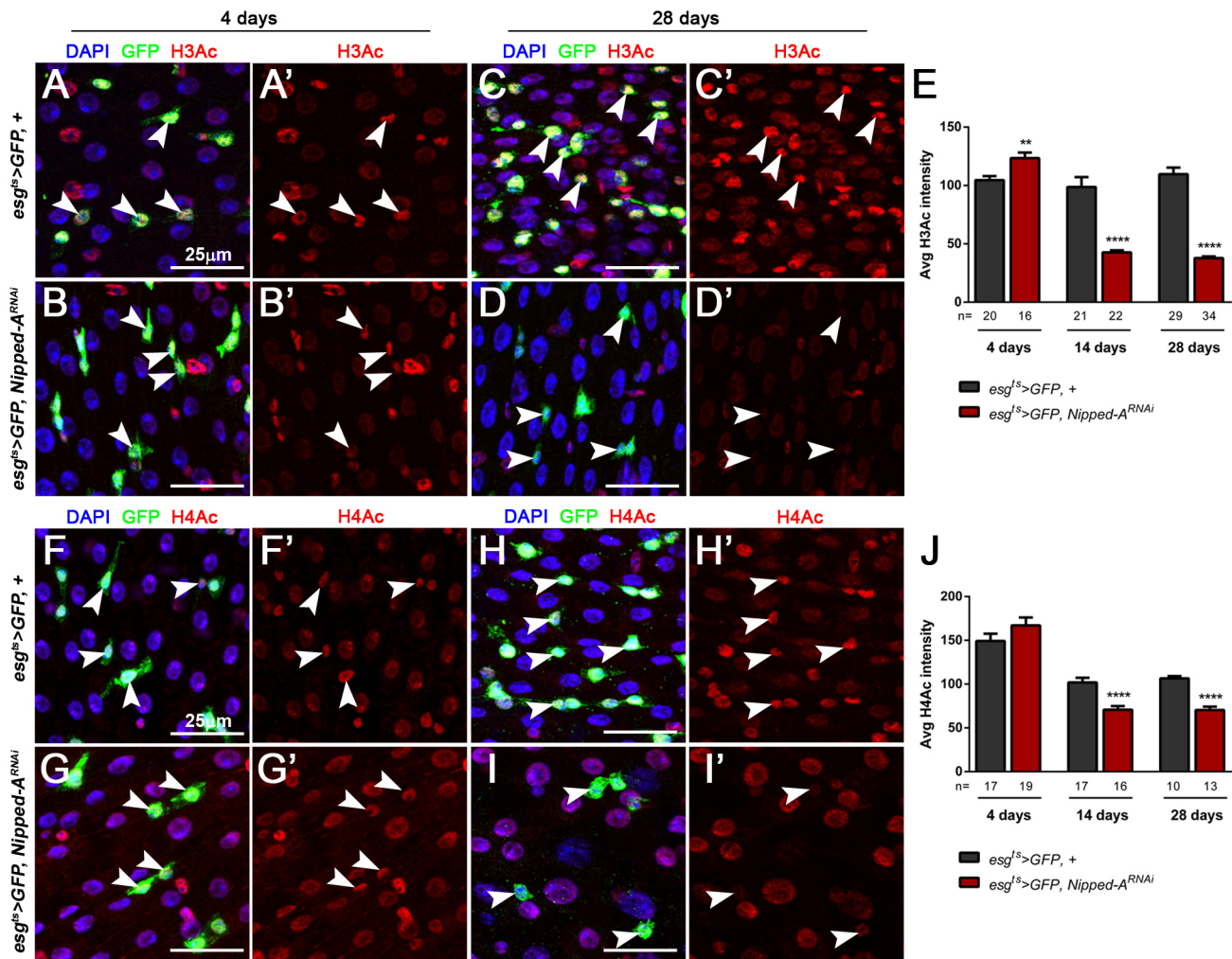
Fig. 7. *Nipped-A* reduction results in lower global acetylation of H3 and H4. (A-D′,F-I′) Immunostainings at 4 days (A-B′,F-G′) and 28 days (C-D′,H-I′) for global H3Ac (A-D′) and global H4KAc (F-I′). Arrowheads point to *esg*-GFP+ cells in A-D′,F-I′. (E,J) Quantification of the staining intensity of H3Ac (E) and H4Ac (J) in the *esg*-GFP+ cells at designated time points. All graphs show the mean±s.e.m. Statistical significance was calculated using the Student's *t*-test; **P<0.01, ****P<0.0001. Asterisks directly above bars indicate a significant difference between this bar and the adjacent control bar on the left.

TRRAP was shown to be essential for MYC to activate its target genes and drive oncogenesis (Liu et al., 2003; Park et al., 2001).

Therefore, it is possible that Nipped-A and Myc interact in a multiprotein complex to drive proliferation, which could possibly explain why overexpression of *Myc* alone is not sufficient to induce hyperproliferation. Ideally this hypothesis could be tested by co-overexpressing *Myc* and *Nipped-A*. Unfortunately, Nipped-A is a large protein (3790 aa), bearing challenges for generating the fly lines needed to answer this question.

Considering that Myc might require Nipped-A to interact with and jointly activate gene expression, it was unexpected to see an upregulation in mRNA expression of most of the tested Myc target genes, as well as *Myc* itself, upon *Nipped-A* knockdown. These results indicate that Myc can transcriptionally activate at least a subset of its targets in the absence of *Nipped-A*. Interestingly, this upregulation of *Myc* as well as other cell cycle genes is not sufficient to drive proliferation of the ISCs. Moreover, additional crucial cell cycle genes were expressed at normal or higher levels after *Nipped-A* knockdown, indicating that the lack of proliferation is not due to a reduction in expression of these genes. Thus, the mechanism by which Nipped-A regulates proliferation in *Drosophila* ISCs seems to be distinct from that of TRRAP in some mammalian stem cell

populations (Bouchard et al., 2001; Li et al., 2004; Tapias et al., 2014; Wurdak et al., 2010).

It is possible that Nipped-A regulates a process or a distinct set of genes that are important for downstream cell cycle events such as cytokinesis. We did notice some nuclei with an aberrant morphology after reducing *Nipped-A* in ISCs and EBs. The morphology was reminiscent of nuclei in *TRRAP*-deficient mouse embryonic fibroblasts, which were characterized by a defective spindle assembly checkpoint and chromosome mis-segregation (Herceg et al., 2001; Li et al., 2004). Consistently, two independent screens identified Nipped-A to be important for mitosis (Echard et al., 2004; Somma et al., 2008). Knocking down *Nipped-A* in S2 cells induced the formation of multi-nucleated cells, indicating problems with cytokinesis (Echard et al., 2004), as well as low microtubule density and impaired chromosome segregation, indicating mitotic spindle instability (Somma et al., 2008). These findings offer an additional explanation, at least in part, for the impaired cell proliferation after *Nipped-A* knockdown, and open an avenue for further investigation.

To date there have been few reports that examined the epigenetic state of the chromatin in ISCs and EBs, and how it is regulated. With regard to proliferation and acetylation, there is a known cross-talk

DEVELOPMENT

between the cell cycle regulatory machinery and proteins regulating histone acetylation (Wang et al., 2001). We show that global acetylation of both H3 and H4 is reduced after 14 and 28 days of *Nipped-A* knockdown. Interestingly, the maintenance of acetylated H3 was found to be important for regulating ISC proliferation as well as ISC identity (Amcheslavsky et al., 2014). Thus, it is tempting to speculate that the reduction of H3Ac upon *Nipped-A* knockdown contributes to the observed loss of ISC identity and proliferation. A recent report found an increase in H3K27Ac at enhancers of genes that were important for oncogenesis after induction of HRas[G12V] in mouse embryonic fibroblasts (MEFs) (Nabet et al., 2015). Also, H3K27Ac has been shown to be upregulated in colon cancer (Karczmarski et al., 2014). Thus, increased levels of H3K27Ac are associated with increased proliferation. Upon *Nipped-A* knockdown this mark is significantly less acetylated. Taken together, Nipped-A seems to maintain histone acetylation in ISCs and EBs. Thus, the increased expression of *Nipped-A* in old ISCs could contribute to aberrant gene expression and excess proliferation in aged midguts.

In summary, using RNA-seq to analyze the transcriptome of young and old ISCs, this work provides new perspectives on endogenous changes in ISCs during aging. With Nipped-A, we have newly identified a factor that becomes endogenously upregulated in ISCs during aging and whose expression level seems to be vital for regulating ISC proliferation, especially under high proliferative stress. Our data demonstrate that Nipped-A is a crucial component required for cell division as the activation of pivotal mitogenic signaling pathways, such as EGFR, is unable to drive proliferation in the absence of Nipped-A. Intriguingly, the key factor involved in cell cycle progression, Myc, can still activate its target genes in the absence of Nipped-A; however, this is not sufficient for ISC proliferation. Additionally, we show that Nipped-A regulates global histone acetylation, suggesting that Nipped-A exerts its function by modulating chromatin accessibility to regulate ISC division and/or ISC identity. Taken together, our findings shed light onto the transcriptional differences that potentially drive ISC aging and, with Nipped-A, uncover a new level of regulating ISC proliferation.

MATERIALS AND METHODS
Drosophila stocks and crosses
The following fly lines were obtained from the Bloomington *Drosophila* Stock Center: w^{1118} (5905), UAS-*Nipped-A*-RNAi (34849), UAS-*N*-RNAi (33611), UAS-*dMyc* (9674) and *yw*, neoFRT 19A (1744). UAS-*Nipped-A*-RNAi fly lines (40789, 52487 and 44781) were obtained from the Vienna *Drosophila* RNAi Center. The following fly lines were generously provided by other labs: *esg*-GAL4, UAS-GFP (N 1099) (S. Hayashi, RIKEN Center for Developmental Biology, Kobe, Japan), *esg*-GAL4, UAS-CD8GFP, *tub*-Gal80[ts] (#5) (*esg[ts]*>GFP; J. Knoblich, IMBA, Vienna, Austria), *NRE*-pRedRabbit (mCherry)/TM6B (S. Bray, University of Cambridge, UK), UAS-*Ras[ACT]* (A. Michelson, NHLBI, Bethesda, MD, USA), hsFLP, FRT19, *tub*-GAL80; *tub*-GAL4, UAS-GFP (H. Jasper, The Buck Institute for Research and Aging, Novato, CA, USA), UAS-*dMyc*-HA (P. Bellosta, University of Milan, Italy).

Flies were maintained on standard feeding medium. The TARGET system (McGuire et al., 2003) was used to conditionally express the desired constructs in the *esg*-GFP+ cells. For RNAi knockdown experiments, virgins from the *esg[ts]*>GFP fly line were crossed with w^{1118} or UAS-*Nipped-A*-RNAi males. Virgins from the *NRE*-pRedRabbit (mCherry), UAS-*N*-RNAi, UAS-*Ras[ACT]* and UAS-*dMyc* fly lines were crossed with *esg[ts]*>GFP or *esg[ts]*>GFP; UAS-*Nipped-A*-RNAi males for the co-expression experiments. All crosses were kept at 18°C and freshly eclosed progeny were collected over two days. Mated females were transferred to 29°C 6-8 days after eclosion and aged at 29°C to desired time points. Flies at 29°C were transferred to fresh medium every 2-3 days.

For MARCM (Wu and Luo, 2007) lineage analysis experiments, virgins from the hsFLP, FRT19, *tub*-GAL80; *tub*-GAL4, UAS-GFP fly line were crossed with *yw*, neoFRT 19A;;UAS-*Nipped-A*-RNAi or *yw*, neoFRT 19A (controls). Flies were kept at 25°C after hatching and 5-7-day-old mated female flies were heat-shocked at 37°C for 45 min to induce clone formation.

FACS, RNA sequencing and qPCR
For the RNA sequencing, flies from the *esg*-GAL4, UAS-GFP (N 1099) fly line were kept at 25°C and the food was changed every two to three days. Cells were isolated from young (6-8 days) and old (59-65 days) midguts and GFP-positive cells were sorted by FACS (FACSAria II cell sorter, BD Biosciences) for the ISC-enriched population as described in Tauc et al. (2014). ISCs from three independent batches of young and old flies were sorted into RNAlater solution (Ambion), snap-frozen in liquid nitrogen and sent to MFT Services (Tübingen) for next-generation RNA sequencing.

The FACS method was also used to quantify the number of GFP+ and GFP+/mCherry+ cells isolated from whole midguts for supplemental experiments (using FACS Canto II, BD Biosciences).

For qPCR experiments, RNA was extracted from sorted ISCs (at least 40,000 cells) using RNAzol B solution (Wak-chemie Medical GmbH) and chloroform, followed by an overnight precipitation with isopropanol. cDNA was generated from template mRNA using the QuantiTect Reverse Transcription kit (Qiagen). Samples were prepared in Power SYBR Green Master Mix (Applied Biosystems) and quantitative PCR was performed using 7300 Real-Time PCR System (Applied Biosystems). A list of all primers used can be found in Table S1.

EdU incorporation assay and chemical feeding experiments
For EdU incorporation assays, flies were placed into empty vials that contained Whatman paper (area ~4 cm^2) wet with a water solution containing 5% sucrose (250 µl) and 100 µM EdU (Baseclick) for 24 h. Whole intestines were then dissected and fixed in 4% PFA for 30 min at room temperature. The rest of the procedure was performed according to the manufacturer's instructions.

For the chemical feeding experiments, the same setup was used as for the EdU experiments; however, instead of EdU, the sucrose solution contained either 5% dextran sulfate sodium (MP Biomedicals) or 25 µg/ml bleomycin (Merck Millipore). Flies were transferred to fresh medium once a day and dissected after 48 h of treatment.

Immunohistochemistry
For Pros and mCherry immunostainings, intestines were fixed in 1× PBS containing 10% formaldehyde for 20 min. Washes were performed using 1× PBS with 0.1% Triton X-100 (PBST) and PBST with 1% BSA used for blocking as well as for dilution of primary and secondary antibodies. For Delta stainings, intestines were fixed in a 1:1 (vol/vol) mixture of 4% PFA in 1× PBS and heptane for 15 min. The PFA solution was then replaced with 100% methanol and the heptane was removed. The intestines were then gradually rehydrated in 1× PBS with 0.1% Triton X-100 (PBST): 75%, 50%, 25% methanol in PBST, washed three times and blocked in PBST with 1% BSA for 1 h.

The following antibodies were used: rabbit anti-GFP (1:500; ab6556), chicken anti-GFP (1:1000; ab13970), rabbit anti-histone H3 (acetyl K27; 1:200; ab4729) (all from Abcam); mouse anti-GFP (1:500; 11814460001 Roche); rat anti-Delta (1:1000; generous gift from M. D. Rand, University of Rochester Medical Center, NY, USA), rabbit anti-living colors DsRed (mcherry; 1:500; 632496, Clontech); rabbit anti-phosphohistone H3 (1:500; 9701, Cell Signaling Technology); rabbit anti-acetyl-histone H3 (1:500; 06-599, Millipore); rabbit anti-acetyl-histone H4 (1:500; 06-866, Millipore); mouse anti-Prospero (1:1000; MR1A, Developmental Studies Hybridoma Bank). The following secondary antibodies (diluted 1:500) were used: Alexa Fluor 488-conjugated goat anti-rabbit or goat anti-mouse (111-545-003 or 115-545-003, respectively), Cy3-conjugated donkey anti-rat (712-165-150) or donkey anti-mouse (715-165-150) and DyLight 594-conjugated donkey anti-rabbit (711-515-152) (all from Dianova); Alexa Fluor 488-conjugated goat anti-chicken (A-11039, ThermoFisher).

Intestines were mounted using Immunoselect Antifading Mounting Medium DAPI (Dianova).

TUNEL staining

Whole intestines were dissected and fixed at room temperature in 1× PBS containing 4% PFA for 30 min. Samples were dehydrated to 100% methanol in four steps, rehydrated in four steps to PBST and washed three times. Samples were fixed a second time with 4% PFA for 15 min, washed with PBST and incubated for 1 h in 1× TdT buffer (Fermentas). This was followed by an overnight incubation at room temperature in 0.5 µM digoxygenin-d′UTP (Roche) and 150 U/ml TdT (Fermentas) in 1× TdT buffer. The samples were washed and the signal was detected by using Cy3-conjugated monoclonal mouse anti-Digoxin (1:500; 200-162-156, Dianova) secondary antibody.

Microscopy and image analysis

An epifluorescent Olympus microscope or a Leica SP5 II microscope was used for analyzing midgut specimens. For confocal microscopy, stacks of images were taken that were then further processed using ImageJ (NIH) and Photoshop (Adobe). For cell counting analyses, two stacks of images (63×) of the posterior midgut were taken per midgut and all cells were counted within a 20,000 µm^2 area per image using ImageJ software. Staining intensity in the esg-GFP$^+$ cells for H3Ac, H4Ac and H3K27Ac was measured using ImageJ by manually circling the stained area within the cell nucleus.

Statistical analysis

Statistical analysis was performed using GraphPad Prism. The Student's t-test (unpaired, two-tailed) was used for comparing differences between mean values. The Chi square test was used to calculate significance for the MARCM analysis.

Competing interests

The authors declare no competing or financial interests.

Author contributions

H.M.T. conceived and performed the experiments, and wrote the manuscript. A.T. assisted with the FACS analysis. P.M. assisted with qPCR experiments. P.P. conceived the experiments, wrote the manuscript, and secured funding.

Data availability

The RNA-seq data reported have been deposited in GEO under Accession Number GSE94394.

Supplementary information

Supplementary information available online at
http://dev.biologists.org/lookup/doi/10.1242/dev.142703.supplemental

References

Amcheslavsky, A., Jiang, J. and Ip, Y. T. (2009). Tissue damage-induced intestinal stem cell division in Drosophila. *Cell Stem Cell* **4**, 49-61.

Amcheslavsky, A., Nie, Y., Li, Q., He, F., Tsuda, L., Markstein, M. and Ip, Y. T. (2014). Gene expression profiling identifies the zinc-finger protein Charlatan as a regulator of intestinal stem cells in Drosophila. *Development* **141**, 2621-2632.

Bardin, A. J., Perdigoto, C. N., Southall, T. D., Brand, A. H. and Schweisguth, F. (2010). Transcriptional control of stem cell maintenance in the Drosophila intestine. *Development* **137**, 705-714.

Biteau, B. and Jasper, H. (2011). EGF signaling regulates the proliferation of intestinal stem cells in Drosophila. *Development* **138**, 1045-1055.

Biteau, B., Hochmuth, C. E. and Jasper, H. (2008). JNK activity in somatic stem cells causes loss of tissue homeostasis in the aging Drosophila gut. *Cell Stem Cell* **3**, 442-455.

Biteau, B., Karpac, J., Supoyo, S., DeGennaro, M., Lehmann, R. and Jasper, H. (2010). Lifespan extension by preserving proliferative homeostasis in Drosophila. *PLoS Genet* **6**, e1001159.

Biteau, B., Hochmuth, C. E. and Jasper, H. (2011). Maintaining tissue homeostasis: dynamic control of somatic stem cell activity. *Cell Stem Cell* **9**, 402-411.

Bonfini, A., Liu, X. and Buchon, N. (2016). From pathogens to microbiota: how Drosophila intestinal stem cells react to gut microbes. *Dev. Comp. Immunol.* **64**, 22-38.

Bouchard, C., Dittrich, O., Kiermaier, A., Dohmann, K., Menkel, A., Eilers, M. and Lüscher, B. (2001). Regulation of cyclin D2 gene expression by the Myc/Max/Mad network: Myc-dependent TRRAP recruitment and histone acetylation at the cyclin D2 promoter. *Genes Dev.* **15**, 2042-2047.

Buchon, N., Broderick, N. A., Chakrabarti, S. and Lemaitre, B. (2009). Invasive and indigenous microbiota impact intestinal stem cell activity through multiple pathways in Drosophila. *Genes Dev* **23**, 2333-2344.

Buszczak, M., Paterno, S. and Spradling, A. C. (2009). Drosophila stem cells share a common requirement for the histone H2B ubiquitin protease scrawny. *Science* **323**, 248-251.

Choi, N.-H., Kim, J.-G., Yang, D.-J., Kim, Y.-S. and Yoo, M.-A. (2008). Age-related changes in Drosophila midgut are associated with PVF2, a PDGF/VEGF-like growth factor. *Aging Cell* **7**, 318–334.

Cordero, J. B., Stefanatos, R. K., Scopelliti, A., Vidal, M. and Sansom, O. J. (2012). Inducible progenitor-derived Wingless regulates adult midgut regeneration in Drosophila. *EMBO J.* **31**, 3901-3917.

de Navascues, J., Perdigoto, C. N., Bian, Y., Schneider, M. H., Bardin, A. J., Martinez-Arias, A. and Simons, B. D. (2012). Drosophila midgut homeostasis involves neutral competition between symmetrically dividing intestinal stem cells. *EMBO J* **31**, 2473-2485.

Echard, A., Hickson, G. R. X., Foley, E. and O'Farrell, P. H. (2004). Terminal cytokinesis events uncovered after an RNAi screen. *Curr Biol* **14**, 1685-1693.

Feser, J. and Tyler, J. (2011). Chromatin structure as a mediator of aging. *FEBS Lett.* **585**, 2041-2048.

Frank, S. R., Schroeder, M., Fernandez, P., Taubert, S. and Amati, B. (2001). Binding of c-Myc to chromatin mediates mitogen-induced acetylation of histone H4 and gene activation. *Genes Dev.* **15**, 2069-2082.

Gause, M., Eissenberg, J. C., Macrae, A. F., Dorsett, M., Misulovin, Z. and Dorsett, D. (2006). Nipped-A, the Tra1/TRRAP subunit of the Drosophila SAGA and Tip60 complexes, has multiple roles in Notch signaling during wing development. *Mol. Cell. Biol.* **26**, 2347-2359.

Guo, L., Karpac, J., Tran, S. L. and Jasper, H. (2014). PGRP-SC2 promotes gut immune homeostasis to limit commensal dysbiosis and extend lifespan. *Cell* **156**, 109-122.

Herceg, Z., Hulla, W., Gell, D., Cuenin, C., Lleonart, M., Jackson, S. and Wang, Z.-Q. (2001). Disruption of Trrap causes early embryonic lethality and defects in cell cycle progression. *Nat Genet* **29**, 206-211.

Jasper, H. (2015). Exploring the physiology and pathology of aging in the intestine of Drosophila melanogaster. *Invertebr Reprod Dev* **59**, 51-58.

Jiang, H., Grenley, M. O., Bravo, M. J., Blumhagen, R. Z. and Edgar, B. A. (2011). EGFR/Ras/MAPK signaling mediates adult midgut epithelial homeostasis and regeneration in Drosophila. *Cell Stem Cell* **8**, 84-95.

Jin, Y., Xu, J., Yin, M.-X. X., Lu, Y., Hu, L., Li, P., Zhang, P., Yuan, Z., Ho, M. S., Ji, H. et al. (2013). Brahma is essential for Drosophila intestinal stem cell proliferation and regulated by Hippo signaling. *eLife* **2**, e00999.

Karczmarski, J., Rubel, T., Paziewska, A., Mikula, M., Bujko, M., Kober, P., Dadlez, M. and Ostrowski, J. (2014). Histone H3 lysine 27 acetylation is altered in colon cancer. *Clin. Proteomics* **11**, 24.

Kirkwood, T. B. L. (2004). Intrinsic ageing of gut epithelial stem cells. *Mech Ageing Dev* **125**, 911-915.

Kusch, T., Guelman, S., Abmayr, S. M. and Workman, J. L. (2003). Two Drosophila Ada2 homologues function in different multiprotein complexes. *Mol. Cell. Biol.* **23**, 3305-3319.

Li, H., Cuenin, C., Murr, R., Wang, Z.-Q. and Herceg, Z. (2004). HAT cofactor Trrap regulates the mitotic checkpoint by modulation of Mad1 and Mad2 expression. *EMBO J* **23**, 4824-4834.

Liu, X., Tesfai, J., Evrard, Y. A., Dent, S. Y. R. and Martinez, E. (2003). c-Myc transformation domain recruits the human STAGA complex and requires TRRAP and GCN5 acetylase activity for transcription activation. *J. Biol. Chem.* **278**, 20405-20412.

Ma, Y., Chen, Z., Jin, Y. and Liu, W. (2013). Identification of a histone acetyltransferase as a novel regulator of Drosophila intestinal stem cells. *FEBS Lett* **587**, 1489-1495.

McGuire, S. E., Le, P. T., Osborn, A. J., Matsumoto, K. and Davis, R. L. (2003). Spatiotemporal rescue of memory dysfunction in Drosophila. *Science* **302**, 1765-1768.

DEVELOPMENT

McMahon, S. B., Van Buskirk, H. A., Dugan, K. A., Copeland, T. D. and Cole, M. D. (1998). The novel ATM-related protein TRRAP is an essential cofactor for the c-Myc and E2F oncoproteins. *Cell* **94**, 363-374.

Micchelli, C. A. and Perrimon, N. (2006). Evidence that stem cells reside in the adult Drosophila midgut epithelium. *Nature* **439**, 475-479.

Murr, R., Vaissiere, T., Sawan, C., Shukla, V., Herceg, Z., Vaissière, T., Sawan, C., Shukla, V. and Herceg, Z. (2007). Orchestration of chromatin-based processes: mind the TRRAP. *Oncogene* **26**, 5358-5372.

Nabet, B., Ó Broin, P., Reyes, J. M., Shieh, K., Lin, C. Y., Will, C. M., Popovic, R., Ezponda, T., Bradner, J. E., Golden, A. A. et al. (2015). Deregulation of the Ras-Erk signaling axis modulates the enhancer landscape. *Cell Rep.* **12**, 1300–1313.

O'Brien, L. E., Soliman, S. S., Li, X. and Bilder, D. (2011). Altered modes of stem cell division drive adaptive intestinal growth. *Cell* **147**, 603-614.

Ohlstein, B. and Spradling, A. (2006). The adult Drosophila posterior midgut is maintained by pluripotent stem cells. *Nature* **439**, 470-474.

Ohlstein, B. and Spradling, A. (2007). Multipotent Drosophila intestinal stem cells specify daughter cell fates by differential notch signaling. *Science* **315**, 988-992.

Orian, A., van Steensel, B., Delrow, J., Bussemaker, H. J., Li, L., Sawado, T., Williams, E., Loo, L. W. M., Cowley, S. M., Yost, C. et al. (2003). Genomic binding by the Drosophila Myc, Max, Mad/Mnt transcription factor network. *Genes Dev.* **17**, 1101-1114.

Park, J., Kunjibettu, S., McMahon, S. B. and Cole, M. D. (2001). The ATM-related domain of TRRAP is required for histone acetyltransferase recruitment and Myc-dependent oncogenesis. *Genes Dev.* **15**, 1619-1624.

Park, J.-S., Kim, Y.-S. and Yoo, M.-A. (2009). The role of p38b MAPK in age-related modulation of intestinal stem cell proliferation and differentiation in Drosophila. *Aging (Albany. NY).* **1**, 637-651.

Perdigoto, C. N., Schweisguth, F. and Bardin, A. J. (2011). Distinct levels of Notch activity for commitment and terminal differentiation of stem cells in the adult fly intestine. *Development* **138**, 4585-4595.

Prober, D. A. and Edgar, B. A. (2000). Ras1 promotes cellular growth in the Drosophila wing. *Cell* **100**, 435-446.

Ren, F., Wang, B., Yue, T., Yun, E.-Y., Ip, Y. T. and Jiang, J. (2010). Hippo signaling regulates Drosophila intestine stem cell proliferation through multiple pathways. *Proc Natl Acad Sci U S A* **107**, 21064-21069.

Ren, F., Shi, Q., Chen, Y., Jiang, A., Ip, Y. T., Jiang, H. and Jiang, J. (2013). Drosophila Myc integrates multiple signaling pathways to regulate intestinal stem cell proliferation during midgut regeneration. *Cell Res* **23**, 1133-1146.

Rera, M., Bahadorani, S., Cho, J., Koehler, C. L., Ulgherait, M., Hur, J. H., Ansari, W. S., Lo, T., Jones, D. L., Walker, D. W. et al. (2011). Modulation of longevity and tissue homeostasis by the Drosophila PGC-1 homolog. *Cell Metab.* **14**, 623-634.

Saffrey, M. J. (2014). Aging of the mammalian gastrointestinal tract: a complex organ system. *Age* **36**, 9603.

Somma, M. P., Ceprani, F., Bucciarelli, E., Naim, V., De Arcangelis, V., Piergentili, R., Palena, A., Ciapponi, L., Giansanti, M. G., Pellacani, C. et al. (2008). Identification of Drosophila mitotic genes by combining co-expression analysis and RNA interference. *PLoS Genet* **4**, e1000126.

Tapias, A., Zhou, Z.-W., Shi, Y., Chong, Z., Wang, P., Groth, M., Platzer, M., Huttner, W., Herceg, Z., Yang, Y.-G. et al. (2014). Trrap-dependent histone acetylation specifically regulates cell-cycle gene transcription to control neural progenitor fate decisions. *Cell Stem Cell* **14**, 632-643.

Tauc, H. M., Tasdogan, A. and Pandur, P. (2014). Isolating intestinal stem cells from adult Drosophila midguts by FACS to study stem cell behavior during aging. *J Vis Exp.* **94**, e52223.

Wang, C., Fu, M., Mani, S., Wadler, S., Senderowicz, A. M. and Pestell, R. G. (2001). Histone acetylation and the cell-cycle in cancer. *Front. Biosci.* **6**, D610-D629.

Wang, L., Karpac, J. and Jasper, H. (2014). Promoting longevity by maintaining metabolic and proliferative homeostasis. *J Exp Biol* **217**, 109-118.

Wu, J. S. and Luo, L. (2007). A protocol for mosaic analysis with a repressible cell marker (MARCM) in Drosophila. *Nat. Protoc.* **1**, 2583-2589.

Wurdak, H., Zhu, S., Romero, A., Lorger, M., Watson, J., Chiang, C.-Y., Zhang, J., Natu, V. S., Lairson, L. L., Walker, J. R. et al. (2010). An RNAi screen identifies TRRAP as a regulator of brain tumor-initiating cell differentiation. *Cell Stem Cell* **6**, 37-47.

Yagi, Y. and Hayashi, S. (1997). Role of the Drosophila EGF receptor in determination of the dorsoventral domains of escargot expression during primary neurogenesis. *Genes Cells* **2**, 41-53.

Zeng, X., Lin, X. and Hou, S. X. (2013). The Osa-containing SWI/SNF chromatin-remodeling complex regulates stem cell commitment in the adult Drosophila intestine. *Development* **140**, 3532-3540.

DEVELOPMENT